RSC Sustainability

ROYAL SOCIETY OF CHEMISTRY

PAPER

View Article Online
View Journal | View Issue

Cite this: *RSC Sustainability*, 2024, **2**, 3311

Chemically recyclable and reprogrammable epoxy thermosets derived from renewable resources†

Tankut Türel, ‡ Özgün Dağlar, ‡ Christos Pantazidis and Željko Tomović *

Epoxy thermosets constitute a significant portion of high-performance plastics due to their excellent thermal and mechanical properties, making them suitable for a wide range of applications. However, traditional epoxy networks are produced from a petroleum-based, reprotoxic and endocrine-disruptor DGEBA and face significant limitations in chemical recycling. Current recycling methods for epoxy systems rely on harsh and non-green conditions, often resulting in a mixture of small molecules and oligomers that are tedious to isolate or repurpose. Consequently, it is crucial to develop bio-based monomers with functional groups that enable the synthesis of fully recyclable polymers. For this purpose, herein, we have employed a bio-based, liquid monomer **C2** derived from vanillin, containing aldehyde, acetal, and oxirane-ring functionalities, which was polymerized under solvent-free, green conditions with bio-derived diamines, resulting in an array of doubly cleavable epoxy thermosets with diverse thermal and mechanical properties. These networks combine the desirable properties of traditional epoxy systems with intrinsic mildly cleavable nature. Remarkably, these thermosets can be fully depolymerized into reusable vanillin and well-defined polyols, or they can be recycled and reprogrammed through a transimination pathway. This innovative approach, combining controlled depolymerization, closed-loop recycling and reprogramming, offers significant potential for sustainable polymer management.

Received 16th July 2024
Accepted 26th September 2024

DOI: 10.1039/d4su00382a

rsc.li/rscsus

Sustainability spotlight

The development of bio-based, recyclable epoxy resins addresses the significant environmental challenges posed by traditional petroleum-derived thermosetting plastics. By integrating cleavable acetal and imine bonds into epoxy networks, our work enables efficient chemical recycling and repurposing under mild conditions. This advancement aligns with the UN Sustainable Development Goals 12 (Responsible Consumption and Production), 13 (Climate Action), 14 and 15 (Life below Water and on Land), by promoting sustainable industrial practices and reducing waste. Our approach contributes to a circular economy by transforming waste materials into high-value products, decreasing the overall carbon footprint, and advancing sustainable polymer management. This innovation is crucial for creating next-generation, high-performance materials that are both sustainable and versatile.

Introduction

In recent decades, thermosetting polymers have become indispensable in various industrial applications and for everyday use, owing to their remarkable thermal and mechanical properties derived from their covalently crosslinked architectures.[1] Among these, epoxy thermosets stand out as a significant component of high-performance thermosets, finding extensive use in a wide range of industries such as in aerospace, automotive, adhesives, coatings, construction, paints, floorings, and wind turbine blades.[2–4]

Traditionally, 75% of epoxy systems are derived from the commercially available diglycidyl ether of bisphenol A (DGEBA), renowned for its excellent properties due to its high aromatic content and rigidity.[5] Nevertheless, DGEBA, being a derivative of bisphenol A (BPA), is a petroleum-based monomer which has raised concerns due to its known reprotoxic and endocrine-disrupting nature,[6,7] prompting the research for bio-based alternatives. Derivatives of bio-derived monomers (*i.e.*, vanillin, 4-hydroxybenzaldehyde, epoxidized soybean oil, furan, *etc.*) have therefore emerged as promising candidates.[8–17]

While traditional epoxy thermosets exhibit superior mechanical and thermal properties, their recycling poses significant challenges due to the existence of strong and irreversible covalent bonds in their structures.[18,19] Epoxy networks are typically cured with amine-based hardeners, which poses a significant challenge for their chemical recycling due to the relatively high bond dissociation energies of C–N bonds (~90–110 kJ mol^{-1}).[20,21] A large proportion of epoxy thermosets and

Polymer Performance Materials Group, Department of Chemical Engineering and Chemistry, Eindhoven University of Technology, Eindhoven, 5600 MB, The Netherlands. E-mail: z.tomovic@tue.nl

† Electronic supplementary information (ESI) available. See DOI: https://doi.org/10.1039/d4su00382a

‡ These authors contributed equally.

their carbon fiber-reinforced composites therefore often ends up in landfills or incineration, leading to resource waste and environmental pollution.[22] Current methods for recycling of epoxy waste include mechanical recycling, pyrolysis, and chemical and thermal degradation.[23–28] However, these methods are energy-intensive and often result in complex mixtures of small molecules and oligomers that cannot be separated, reused, or upcycled.[24,25] Therefore, these methods can be rather called degradation instead of controlled depolymerization.[4]

In the light of the need to reduce the carbon footprint of plastics, there is a growing consciousness in designing innovative monomers and polymers to enable circularity.[29–35] Incorporating cleavable imine or acetal bonds into polymer and epoxy networks offers a promising approach.[36–52] These bonds facilitate controlled depolymerization under mild acidic conditions, allowing for efficient chemical recycling. In our previous study, we demonstrated an innovative array of liquid epoxy monomers containing both aldehyde and acetal moieties.[38] When cured with diamines, such monomers form acetal and imine-functional doubly cleavable epoxy networks with tensile strength in the range between 50 and 70 MPa. We also showed that such systems could be repurposed into mixtures of well-defined polyols which are suitable for upcycling into polyurethanes.[38]

Transimination, on the other hand, involves the addition of excess amines to the network, partially cleaving the network resulting in soluble amine-end capped oligomers which enable closed-loop recycling of the epoxy networks.[53–55] However, reprogramming the thermal and mechanical properties of such epoxy systems *via* the transimination pathway has never been demonstrated previously. This procedure can be integral to a circular economy strategy, where materials are continuously repurposed and reprogrammed to meet new demands, thereby extending their lifecycle. Reprogramming can also enhance the value of materials by imparting new and desirable properties, transforming lower-value waste into higher-value products. By reducing the need for new polymer production and utilizing existing materials, the overall carbon footprint will undoubtedly be decreased.

Herein, we have developed an array of recyclable, high-performance epoxy networks with high bio-based content by exclusively utilizing the vanillin-based **C2** monomer and bio-based diamines (*i.e.*, 1,5-diaminopentane (**PDA**), 1,8-diamino-*p*-menthane (**MDA**) and furan-2,5-diyldimethanamine (**FDA**))[56] under solvent-free conditions (Scheme 1). The obtained bio-based recyclable epoxy networks exhibited elastomeric to rigid behaviour with tensile strengths ranging from 24 to 58 MPa and elongation at break values between 8% and 79%. More importantly, these networks were recyclable through two different approaches: first, by simultaneous acidic hydrolysis of imine and acetal groups, and second, by transimination of imine groups. Acidic hydrolysis of acetal and imine groups enabled the recovery of vanillin in high yield and purity, providing an easy and elegant pathway to recover this initial building block, whose production from lignin typically requires harsh conditions and results in low yields.[57] As a byproduct of the acidic depolymerization, a mixture of valuable bio-based well-defined polyols was obtained, which could be used for upcycling into polyurethanes.[38] In addition, transimination of the networks was performed to achieve closed-loop recycling without any performance loss. Moreover, the characteristics of the networks were altered through reprogramming *via* transimination. Such synergistic recycling and repurposing strategies for epoxy systems offer significant potential for sustainable polymer management.

Results and discussion

The synthesis of monomer **C2** was conducted as described in our previous work, in which **C2** was obtained *via* a catalyst-free, click-type addition reaction between vanillin and a vinyl ether functional epoxy precursor, 2-((2-(vinyloxy)ethoxy)methyl)oxirane, **VE2**.[38] (Scheme S1, Fig. S1 and S2†).

To check the stability of the acetal group in the presence of amines, we conducted a model reaction using **C2** and furfuryl amine under bulk conditions at 100 °C (Scheme S2†). We observed that the amine exhibited selectivity towards the aldehyde and epoxy ring, and the reaction was completed within approximately 30 minutes, as evidenced by the disappearance of the proton signals of the epoxy ring at 3.12 and 2.77 ppm and aldehyde proton at 9.82 ppm, with the acetal groups at 5.52 ppm remaining intact (Fig. S3†).

All networks were obtained by curing the **C2** monomer under bulk, solvent-free, single-step conditions with bio-derived diamines **PDA**, **MDA**, and **FDA** (Scheme 1).[56] A homogeneous mixture of monomers was heated to 100 °C under a N_2 flow for 24 h. We additionally fabricated a 3-ply carbon fiber reinforced composite utilizing the **C2FDA** network to obtain **C2FDA-CFC**. Fig. 1 shows the FTIR spectra of the cured networks and monomers. Upon curing, the aldehydic carbonyl stretching vibration at 1682 cm^{-1} disappeared, and an imine peak appeared at 1643 cm^{-1}. Additionally, the emergence of broad –O–H stretching peaks between 3600 and 3100 cm^{-1}, a significant decrease in the intensity of the C–H stretching of the oxirane ring at 3060 cm^{-1} and a decrease in the intensity of the C–O stretching of the oxirane ring at 910 cm^{-1} indicated successful network formation. The peak observed at 1265 cm^{-1}, indicating the presence of the acetal structure, remained constant throughout the polymerization process, demonstrating the stability of the acetals during polymerization, which is in line with our model experiments.

Immersion of the synthesized networks **C2PDA** and **C2FDA** in various organic solvents (*n*-hexane, diethyl ether, tetrahydrofuran, ethyl acetate, acetone, ethanol, and dimethylformamide) and water for 3 days at room temperature demonstrated their resistance, evidenced by relatively high gel fractions and low swelling degrees (Tables S1, S2, Fig. S4 and S5†). Importantly, these networks exhibited stability towards water, with no observed hydrolysis. This was confirmed by the identical FTIR spectra of the water-immersed networks compared to the pristine networks (Fig. S6 and S7†).

The thermal properties of the networks were analyzed using thermogravimetric analysis (TGA) and differential scanning calorimetry (DSC) under a N_2 atmosphere. Fig. 2A and B present the TGA and DSC thermograms of the epoxy networks, respectively. All the networks demonstrated good thermal stability

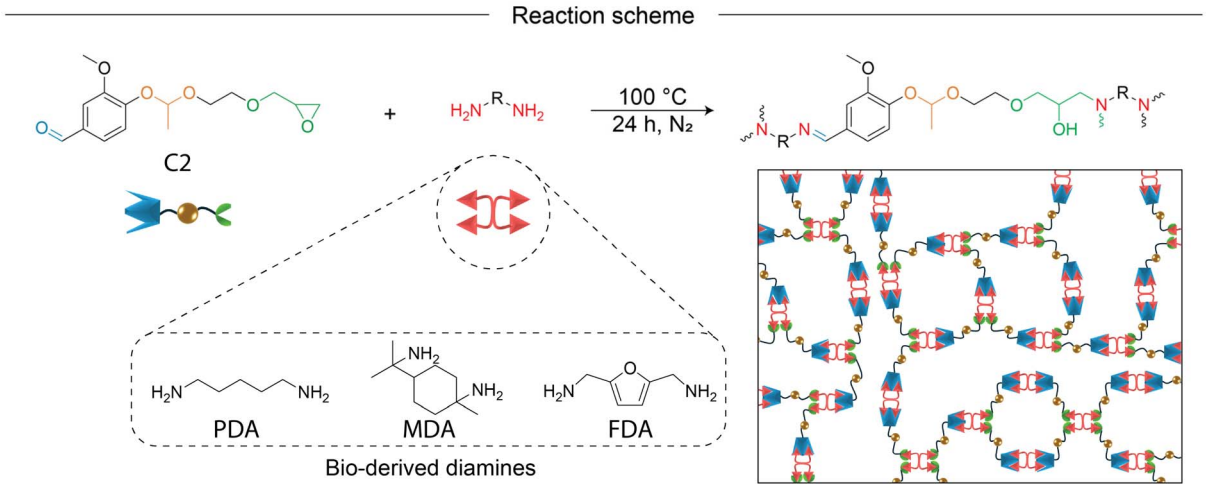

Scheme 1 Synthesis of bio-based, doubly-cleavable epoxy networks.

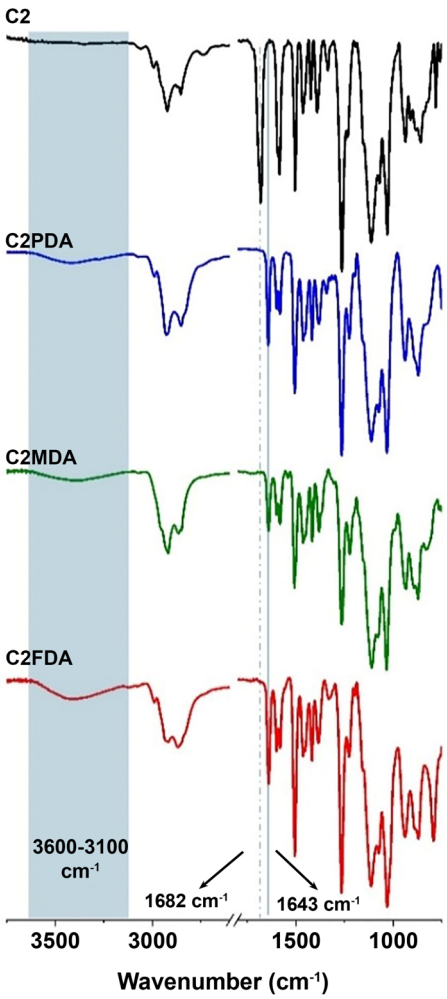

Fig. 1 FTIR spectra of the C2 monomer and the cured networks.

under N_2. The onset degradation temperatures ($T_{d5\%}$) for these networks ranged between 265 and 273 °C. Additionally, a 30% weight loss ($T_{d30\%}$) was observed between 315 and 341 °C (Table 1). Moreover, the char residue of **C2FDA** was 43.4%, significantly higher than those of **C2PDA** (22.9%) and **C2MDA** (15.3%) at 800 °C. This increase in char residue is attributed to the higher aromatic content in **C2FDA**. The glass transition temperatures obtained from DSC ($T_{g,DSC}$) ranged from 30 °C to 56 °C (Fig. 2B and Table 1). For instance, **C2PDA**, which contains linear, flexible pentanediamine (**PDA**) moieties, had a T_g of 30 °C. Substituting this diamine with more rigid cycloaliphatic (**MDA**) or aromatic (**FDA**) diamines increased the rigidity of the backbone, elevating the T_g to 46 °C for **C2FDA** and 56 °C for **C2MDA**.

The thermomechanical properties of the networks were determined using DMA (Fig. 2C, S8,† and Table 1). The storage moduli at 30 °C (E_{30}') for the **C2PDA**, **C2MDA**, and **C2FDA** networks were 1.7, 2.4, and 3.4 GPa, respectively. As the flexibility of the diamine hardener decreased, by substituting the linear **PDA** with the more rigid cycloaliphatic **MDA** or aromatic **FDA**, the stiffness of the material increased significantly, resulting in a higher storage modulus. The maxima of the tanδ *versus* temperature plots were used to determine the T_g values of the networks (Fig. 2C and Table 1). The T_g values obtained from DMA ranged from 44 to 74 °C and followed the same trend as those obtained from DSC. In addition, carbon fiber reinforcement led to a significant enhancement in E_{30}' (7.2 GPa) along with a slight rise in the T_g for **C2FDA-CFC** (72 °C) as compared with its matrix, **C2FDA**.

The mechanical characterization of the epoxy networks was performed using tensile tests (Fig. 2D and S9†). The tensile strength of the networks ranged from 24.2 ± 1.3 to 58.0 ± 1.5 MPa, with the elongation at break ranging from 7.8 ± 0.9% to 79.2 ± 1.4%. Specifically, the **C2PDA** network exhibited a tensile strength of 24.2 ± 1.3 MPa and an elongation at break of 79.2% ± 1.4%. Replacing the hardener **PDA** with more rigid ones, such as **MDA** and **FDA**, resulted in significant changes in mechanical properties. The **C2FDA** network had the highest tensile strength at 58.0 ± 1.5 MPa, with an elongation at break of 11.5 ± 0.5%, while the **C2MDA** network showed a tensile strength of 53.4 ± 0.8 MPa and an elongation at break of 7.8 ± 0.9%. The Young's modulus of **C2FDA** was 2.0 ± 0.1 GPa, whereas that of **C2MDA** and **C2PDA** was 1.7 ± 0.1 GPa and 1.0 ±

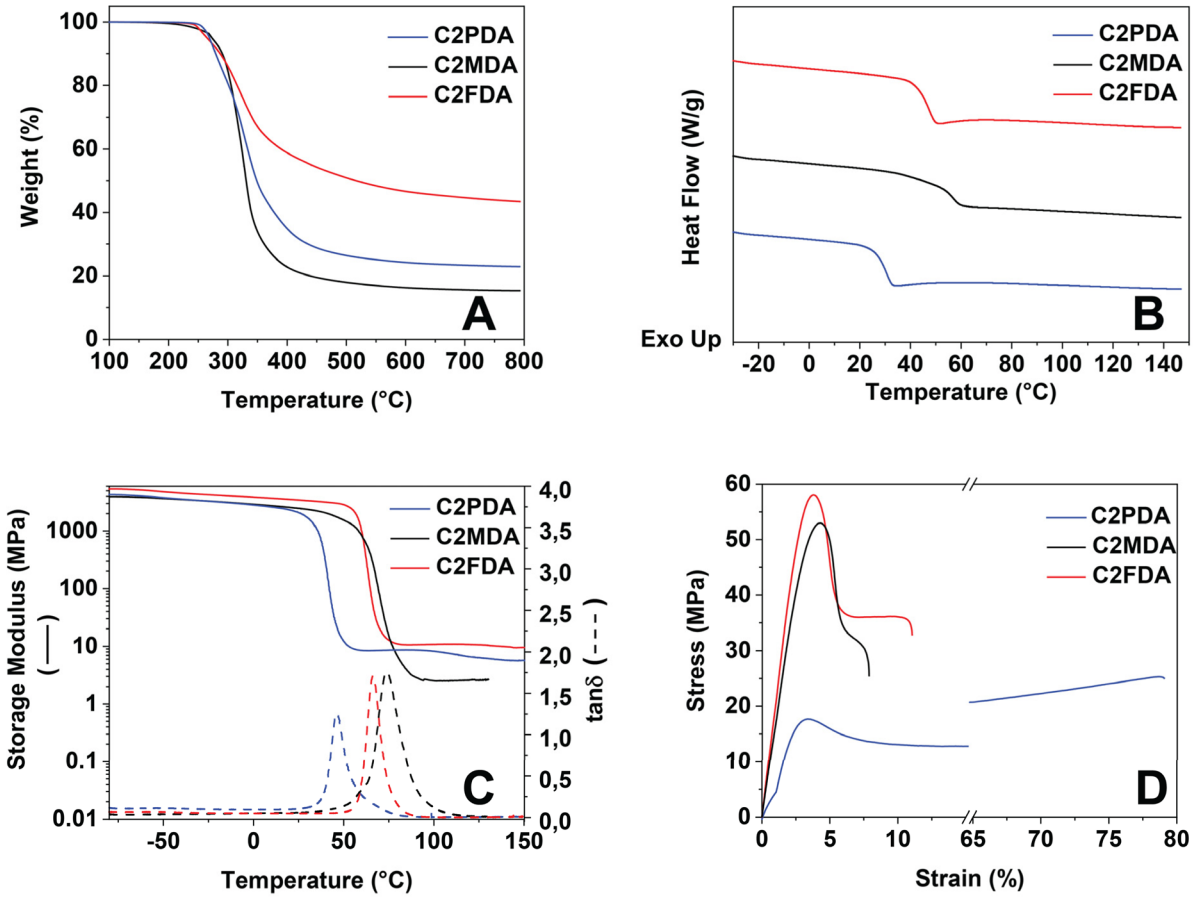

Fig. 2 Thermal, thermomechanical and mechanical characterization of the epoxy networks: TGA (A), DSC (B), DMA (C), tensile tests (D).

0.1 GPa, respectively. This clearly indicated that using an aromatic amine hardener resulted in stiffer networks, which supports the observed trend in storage modulus. On the other hand, **C2FDA-CFC** exhibited a Young's modulus of 8.8 GPa and a tensile strength of 240.0 MPa (Fig. S9†). To gain a more comprehensive insight into the interface between the carbon fiber and the network, we conducted SEM analysis on the original and fractured fibers. The SEM images illustrated that the fibers were thoroughly coated with the epoxy network (Fig. S10†), suggesting a good interaction between the network and carbon fibers, potentially through π–π stacking.

Controlled depolymerization

It is well known that imine and acetal groups are susceptible to acidic hydrolysis.[58,59] While HCl is commonly employed in the hydrolysis of many polyimine and acetal-based systems, its high corrosivity towards metals, skin, and the respiratory tract makes it less suitable for many practical applications. As an alternative, we have employed orthophosphoric acid (1 M) in the presence of a bio-based solvent, Me-THF (20 wt%).

As a proof of concept, the **C2FDA** and **C2PDA** networks were hydrolysed under these conditions (Fig. 3). The hydrolysis was performed at 50 °C, achieving complete solubilization of the

Table 1 Properties of the epoxy networks[a]

	Bio-based content (wt%)[b]	$T_{d1\%}$ (°C)	$T_{d5\%}$ (°C)	$T_{d30\%}$ (°C)	R_{800} (%)	T_g (DSC, °C)	T_g (DMA, °C)	E_{30}' (GPa)	E_{100}' (MPa)	E (GPa)	σ_m (MPa)	ε_b (%)
C2PDA	92.1	253	269	320	22.9	30	44	1.7	8.2	1.0 ± 0.1	24.2 ± 1.3	79.2 ± 1.4
C2MDA	93.1	224	273	315	15.3	56	74	2.4	2.5	1.7 ± 0.1	53.4 ± 0.8	7.8 ± 0.9
C2FDA	92.5	245	265	341	43.4	46	66	3.4	10.8	2.0 ± 0.1	58.0 ± 1.5	11.5 ± 0.5

[a] $T_{d1\%}$, $T_{d5\%}$ and $T_{d30\%}$: temperatures of 1%, 5% and 30% weight loss, respectively. R_{800}: char residue at 800 °C. T_g (DSC) and T_g (DMA): glass transition temperatures obtained from DSC and DMA (maxima of the tanδ curve), respectively. E_{30}' and E_{100}': storage moduli at 30 °C and 100 °C, respectively, obtained from DMA. E: Young's modulus, σ_m: ultimate tensile strength, ε_b: elongation at break. [b] The bio-based weight content is calculated based on the maximum achievable values, assuming that vanillin, ethylene glycol, epichlorohydrin, 1,5-diaminopentane, 1,8-diamino-*p*-menthane, and furan-2,5-diyldimethanamine are sourced from bio-renewable resources. While these compounds can also be obtained from non-bioresources, our calculations are based on their biobased origins.

network within 30 minutes. After that, the Me-THF layer was separated from the aqueous layer, and the aqueous phase was further extracted with ethyl acetate. The organic layers were combined, and upon solvent evaporation, vanillin was obtained in a high yield (≥95%) (Fig. S11†). The collected aqueous phase was neutralized with 1 M NaOH, and after removal of water using a rotary evaporator, the aqueous phase was re-dissolved in DMF. Insoluble phosphate salts were filtered out, and after evaporating the DMF, a well-defined polyol mixture was obtained (Fig. 3, S12, Tables S3 and S4†). ^{1}H NMR spectra also revealed that the polyol mixtures do not have any imine, aldehyde or acetal species, proving a complete depolymerization (Fig. S13 and S14†).

Recovering carbon fibers from composites is crucial due to the high cost and energy-intensive nature of carbon fiber production.[60] Recycling allows for the repurposing of these premium-quality fibers for various applications. Traditionally, carbon fiber recovery from thermosets is a tedious process that significantly degrades fiber quality.[61] In this context, the carbon fiber reinforced **C2FDA-CFC** composite was exposed to 1 M H_3PO_4/Me-THF at 50 °C for 1 hour. This mild recovery method is essential for preserving the original structure of the virgin carbon fibers (Fig. S15†). As shown in the SEM images (Fig. S16†), the fibers maintained pristine quality after acid treatment. This proof-of-concept study demonstrates the potential for chemical recycling of polymer composites using this approach.

Closed-loop recycling through transimination

Another interesting opportunity in the case of imine groups is their ability to react with other amines, thereby replacing the connected amine group through transimination. Utilizing this property, the introduction of excess amines can help solubilize imine-containing networks. As a proof of concept, the networks **C2FDA** and **C2PDA** were dissolved by the addition of excess of their constituent amines **FDA** and **PDA**. In both cases, solubilization was complete within 30 minutes at 50 °C. The additional feed of the other constituent monomer **C2** by protecting the initial stoichiometry between the monomers resulted in the formation of a recycled network with identical thermal and mechanical properties, achieving zero waste (Fig. 4A, S17, and S18†).

Reprogramming through transimination

Transimination, as mentioned above, can be an interesting strategic tool for recycling materials in a closed-loop manner by utilizing identical monomers with pristine polymers. Additionally, this strategy can be employed for reprogramming and repurposing networks through the incorporation of strategically chosen diamines, thereby contributing to sustainable development. For this purpose, we selected **C2PDA** for our reprogramming studies. Initially, **C2PDA** was solubilized with the addition of excess **FDA** monomer in THF to obtain soluble oligomers. Subsequently, an additional feed of **C2** was introduced to yield a reprogrammed **C2PDAFDA** network (Fig. 4B). The thermal and mechanical properties of this network were intermediate between those of the **C2PDA** and **C2FDA** polymers, thus achieving a reprogrammed network. For example, the $T_{d30\%}$, R_{800}, and T_g (measured by DSC) were 331 °C, 34.1%, and 34 °C, respectively, which were higher than those of **C2PDA** but lower than those of **C2FDA**. Similarly, the mechanical properties

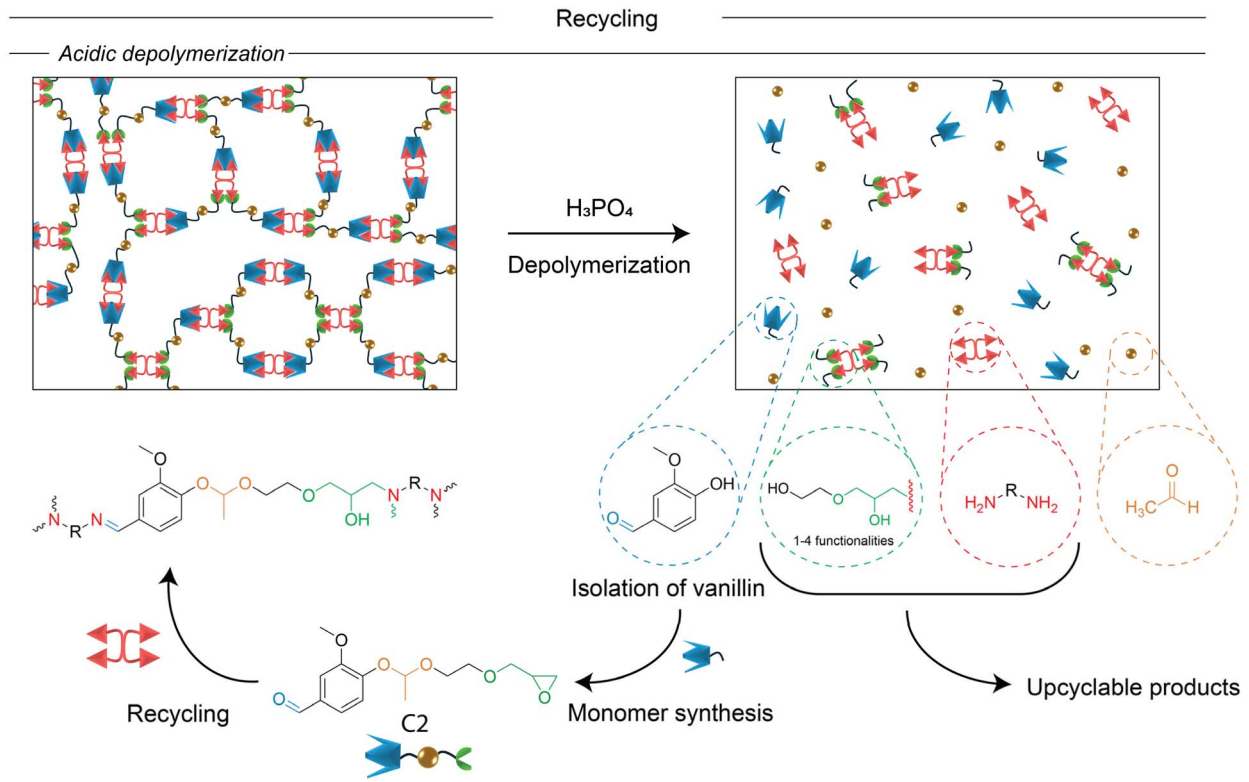

Fig. 3 Illustration of the recycling of designed epoxy networks utilizing controlled acidic depolymerization with 1 M H_3PO_4 solution.

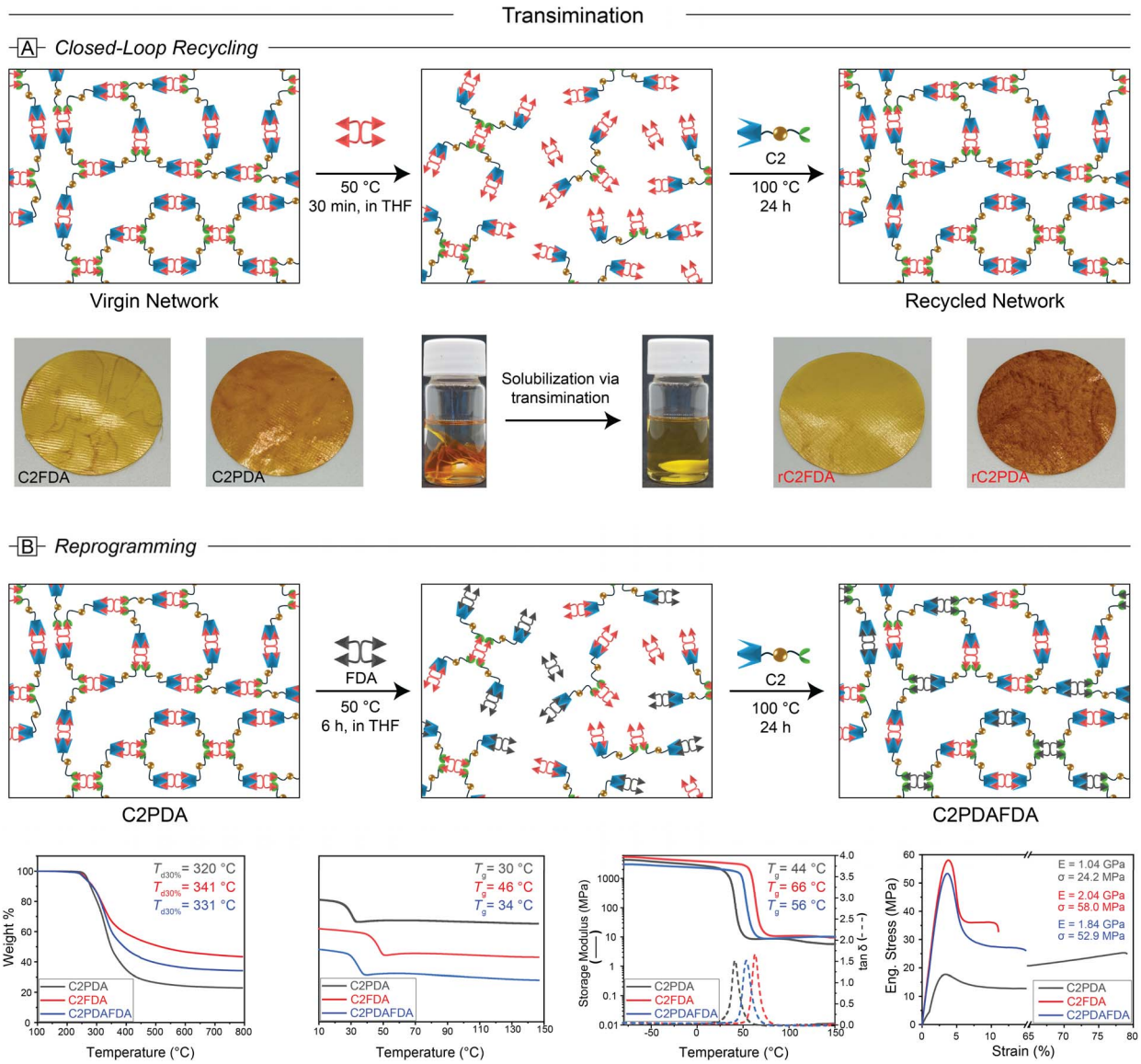

Fig. 4 (A) Illustrative representation of the closed-loop recycling concept *via* transimination, along with photographs of the original, solubilized, and recycled networks. (B) Synthesis of the **C2PDAFDA** network using the reprogramming approach, with comparative results from TGA, DSC, DMA, and tensile tests.

showed enhancement, with a tensile strength of 52.9 MPa and a Young's modulus of 1.8 GPa, compared to the mechanical properties of **C2PDA**, which had a tensile strength of 24.2 MPa and a Young's modulus of 1.0 GPa (Fig. 4B, S19†).

Conclusions

In this study, we have successfully developed a series of recyclable, high-performance epoxy networks with high bio-content, utilizing the vanillin-based **C2** monomer and bio-based diamines (**PDA**, **MDA** and **FDA**) under solvent-free, green conditions. These epoxy networks exhibited a range of mechanical properties from elastomeric to rigid behavior, with tensile strengths spanning from 24 to 58 MPa and elongation at break values from 8% to 79%. Importantly, these networks are recyclable through two distinct pathways: simultaneous acidic hydrolysis of imine and acetal groups and transimination of imine groups. The acidic hydrolysis approach allowed for the efficient recovery of vanillin in high yield and purity, along with a mixture of bio-based polyols suitable for upcycling into polyurethanes. The transimination pathway enabled closed-loop recycling without any purification steps and without any performance loss, as well as facilitated the reprogramming of the networks' thermal and mechanical properties by incorporating different diamines.

Our findings underscore the potential of integrating cleavable bonds into epoxy networks to achieve efficient chemical recycling and extend the lifecycle of materials. This approach not only addresses the environmental challenges associated with traditional thermosetting plastics but also aligns with the principles of a circular economy by enabling the continuous repurposing and reprogramming of materials. By reducing the

need for new polymer production and utilizing existing materials, our work contributes to decreasing the overall carbon footprint and advancing sustainable polymer management. The synergistic strategies demonstrated here pave the way for the development of next-generation, sustainable, high-performance polymers with potential for various industrial applications.

Experimental section

Materials

Vanillin (99%), (±)-epichlorohydrin, (≥99%), ethylene glycol vinyl ether (97%), tetrabutylammonium bromide (TBAB, ≥98%), furfurylamine (≥99%), 1,8-diamino-*p*-menthane (85%, **MDA**), *ortho*-phosphoric acid (H_3PO_4, 99%) and sodium hydroxide (NaOH, ≥97%) were procured from Merck and utilized without further purification. 1,5-Diaminopentane (98%, **PDA**) was sourced from ABCr GmbH, while furan-2,5-diyldimethanamine (95%, **FDA**) was purchased from BLD Pharmaceuticals. Ethyl acetate (EA), dimethylformamide (DMF) and toluene were purchased from Biosolve B.V. 2-Methyltetrahydrofuran (Me-THF) was purchased from TCI. Carbon fibers (S-CF-22-210Pro) with a Young's modulus of 240 GPa, tensile strength of 4.1 GPa, and elongation at break of 1.8% were obtained from EasyComposites. Deuterated $CDCl_3$ was obtained from Cambridge Isotope Laboratories for ^{1}H NMR and ^{13}C NMR analyses. 2-((2-(Vinyloxy)ethoxy)methyl)oxirane (**VE2**) and 3-methoxy-4-(1-(2-(oxiran-2-ylmethoxy)ethoxy)ethoxy) benzaldehyde (**C2**) were synthesized using reported procedures.

Methods

^{1}H NMR and ^{13}C NMR spectra were recorded on a Bruker UltraShield (400 MHz) using $CDCl_3$ or DMSO-d_6 as the solvent. Mass spectrometry of the compounds was performed with an LCQ Fleet ESI-MS (Thermo Fisher Scientific). FTIR spectra were recorded on a Thermo Scientific NICOLET iS20 FTIR spectrometer as an average of 8 scans over the wavenumber range of 450–4000 cm^{-1}.

Swelling measurements and gel fraction tests were performed in several organic solvents (*e.g.*, *n*-hexane, diethyl ether, dichloromethane, and tetrahydrofuran) and water for 3 days at room temperature utilizing a static method. Swelling ratios were calculated using eqn (1), where q represents the swelling ratio, W_0 the initial weight of the network, and W_s the weight of the swollen network.[62]

$$q = 100 \times \frac{W_s - W_0}{W_0} \quad (1)$$

Gel fractions were calculated using eqn (2), where ϕ stands for the gel fraction, W_0 is the initial weight of the polymer, and W_1 is the weight after drying.[62]

$$\phi = 100 \times \frac{W_1}{W_0} \quad (2)$$

Thermogravimetric analyses were conducted utilizing a TA Instruments TGA550, by heating samples (~10 mg) from 100 to 800 °C under an N_2 atmosphere.

DSC measurements were carried out with a TA Instruments Q2000, where samples (~10 mg) were placed in an aluminum-hermetic pan. The experiments were carried out from −50 to 150 °C. The heating rate was maintained at 10 °C min^{-1}, while the cooling rate was set to 5 °C min^{-1}. Glass transition temperatures were determined by taking the midpoint of the reversible endotherm of the second heating.

Dynamic Mechanical Analysis (DMA) measurements were conducted using a TA Instruments DMA850. The experiments were carried out from −80 °C to 150 °C at a heating rate of 3 °C min^{-1} under an oscillatory strain of 0.1% and a frequency of 1 Hz with a preload force of 0.05 N. The glass transition temperature (T_g) was identified as the peak value of tanδ.

Tensile tests were conducted using a Zwick/Roell Intelligent testing machine equipped with a 1 kN load cell, dumbbell-shaped specimens (effective length: 12 mm, width: 2 mm, and measured thickness around 1.0 mm) at a strain rate of 10 mm min^{-1} and a pre-load of 0.05 N. The Young's modulus was determined by calculating the slope of the derivative of the stress–strain curves from 0.1 to 1% strain. To ensure accuracy and determine the experimental error, three replicates were tested.

The surface morphology of the carbon fibers and the interface between the carbon fibers and the epoxy matrix were examined using Scanning Electron Microscopy (SEM, FEI Quanta 200 3D) at an acceleration voltage of 10 kV. Prior to imaging, the samples underwent gold sputtering (40 mA, 40 seconds).

Preparation of epoxy networks and the composite

Epoxy networks were prepared under solvent-free conditions by heating a homogeneous mixture of monomers in a PTFE mold to 100 °C in an inert environment for 24 h.

C2PDA. The **C2PDA** network was prepared by homogenizing a bulk mixture of **C2** (3.50 g, 11.8 mmol) and **PDA** (0.91 g, 8.9 mmol) at room temperature. The resulting liquid was cured in a nitrogen oven at 100 °C for 24 h.

C2MDA. The **C2MDA** network was prepared by homogenizing a bulk mixture of **C2** (3.50 g, 11.8 mmol) and **MDA** (1.51 g, 8.9 mmol) at room temperature. The resulting liquid was cured in a nitrogen oven at 100 °C for 24 h.

C2FDA. The **C2FDA** network was prepared by homogenizing a bulk mixture of **C2** (3.50 g, 11.8 mmol) and **FDA** (1.12 g, 8.9 mmol) at room temperature. The resulting liquid was cured in a nitrogen oven at 100 °C for 24 h.

C2FDA-CFC. The **C2FDA-CFC** composite was prepared by homogenizing a bulk mixture of **C2** (4 g) and **FDA** (1.28 g) at room temperature in the presence of 3-ply carbon-fiber cloth. The resulting mixture was cured in a nitrogen oven at 100 °C for 24 h. Subsequently, the obtained composite was further pressed at 100 °C under a pressure of 10 kN for 1 hour and then placed in a 80 °C vacuum oven for 12 h.

Controlled acidic depolymerization of epoxy networks

The network film (4.38 g for **C2FDA**, 4.43 g for **C2PDA**) of either **C2FDA** or **C2PDA** was cut into small pieces and dispersed in 50 mL of a solvent mixture containing Me-THF/1 M H_3PO_4 (2/8 by volume). This mixture was heated to 50 °C until a clear

solution was obtained, which took roughly 30 minutes. Subsequently, the Me-THF layer was separated, and the acidic aqueous phase was further extracted with EA (2 × 30 mL). The EA layer was separated and combined with the Me-THF layer and dried over $MgSO_4$. After filtration and evaporation of the organic solvent, vanillin was obtained as a pure solid (1.75 g, 97.4% yield for **C2FDA**; 1.79 g, 95% yield for **C2PDA**).

The remaining acidic aqueous solution, free of vanillin, was neutralized with 1 M NaOH, and water was evaporated under reduced pressure. The solid residue was sonicated in DMF and then filtered to remove DMF insoluble phosphate salts. Evaporation of the organic solvent yielded a viscous liquid containing a mixture of the constituent diamine and well-defined polyols.

The same procedure was applied for depolymerization of the **C2FDA-CFC** composite.

Closed-loop recycling and reprogramming through transimination

rC2PDA. 1.5 g of the original **C2PDA** network was dispersed in 10 mL of THF in the presence of 0.5 g of **PDA** (4.9 mmol) at 50 °C. After 15 minutes, the entire material dissolved. **C2** (1.93 g, 6.5 mmol) was then added to this solution, and the mixture was transferred to a PTFE mold. The amount of THF was first minimized by applying a N_2 flow to the solution. The mold was then transferred to a N_2 oven at 100 °C. Further drying of the film was performed at 80 °C in a vacuum oven.

rC2FDA. 1.5 g of the original **C2FDA** network was dispersed in 10 mL of THF in the presence of 0.5 g of **FDA** (4.0 mmol) at 50 °C. After 15 minutes, the entire material dissolved. **C2** (1.57 g, 5.3 mmol) was then added to this solution, and the mixture was transferred to a PTFE mold. The amount of THF was first minimized by applying a N_2 flow to the solution. The mold was then transferred to a N_2 oven at 100 °C. Further drying of the film was performed at 80 °C in a vacuum oven.

C2PDAFDA. 1.5 g of the original **C2PDA** network was dispersed in 10 mL of THF in the presence of 0.5 g of **FDA** (4.0 mmol) at 50 °C. After 6 h, the entire material dissolved. **C2** (1.57 g, 5.3 mmol) was then added to this solution, and the mixture was transferred to a PTFE mold. The amount of THF was first minimized by applying a N_2 flow to the solution. The mold was then transferred to a N_2 oven at 100 °C. Further drying of the film was performed at 80 °C in a vacuum oven.

Data availability

The data supporting this article have been included as part of the ESI.†

Conflicts of interest

There are no conflicts to declare.

References

1 S. Ma and D. C. Webster, *Prog. Polym. Sci.*, 2018, **76**, 65–110, DOI: **10.1016/j.progpolymsci.2017.07.008**.
2 A. Shundo, S. Yamamoto and K. Tanaka, *JACS Au*, 2022, **2**, 1522–1542, DOI: **10.1021/jacsau.2c00120**.
3 G. Gibson, *Epoxy Resins. Brydson's Plastics Materials*, Elsevier, 8th edn, 2017, 773–797. DOI: **10.1016/B978-0-323-35824-8.00027-X**.
4 T. Türel, Ö. Dağlar, F. Eisenreich and Ž. Tomović, *Chem.–Asian J.*, 2023, **18**, e202300373, DOI: **10.1002/asia.202300373**.
5 S. Kumar, S. Krishnan, S. Mohanty and S. K. Nayak, *Polym. Int.*, 2018, **67**, 815–839, DOI: **10.1002/pi.5575**.
6 H. Okada, T. Tokunaga, X. Liu, S. Takayanagi, A. Matsushima and Y. Shimohigashi, *Environ. Health Perspect.*, 2008, **116**, 32–38, DOI: **10.1289/ehp.10587**.
7 P. Fenichel, N. Chevalier and F. Brucker-Davis, *Ann. Endocrinol.*, 2013, **74**, 211–220, DOI: **10.1016/j.ando.2013.04.002**.
8 M. Fache, B. Boutevin and S. Caillol, *Eur. Polym. J.*, 2015, **68**, 488–502, DOI: **10.1016/j.eurpolymj.2015.03.050**.
9 Y. Hao, L. Zhong, T. Li, J. Zhang and D. Zhang, *ACS Sustainable Chem. Eng.*, 2023, **11**, 11077–11087, DOI: **10.1021/acssuschemeng.3c01337**.
10 M. Zhi, X. Yang, R. Fan, S. Yue, L. Zheng, Q. Liu and Y. He, *ACS Appl. Polym. Mater.*, 2023, **5**, 1312–1324, DOI: **10.1021/acsapm.2c01863**.
11 H. Memon, H. Liu, M. A. Rashid, L. Chen, Q. Jiang, L. Zhang, Y. Wei, W. Liu and Y. Qiu, *Macromolecules*, 2020, **53**, 621–630, DOI: **10.1021/acs.macromol.9b02006**.
12 X.-L. Zhao, Y.-Y. Liu, Y. Weng, Y.-D. Li and J.-B. Zeng, *ACS Sustainable Chem. Eng.*, 2020, **8**, 15020–15029, DOI: **10.1021/acssuschemeng.0c05727**.
13 Y.-Y. Liu, J. He, Y.-D. Li, X.-L. Zhao and J.-B. Zeng, *Compos. Commun.*, 2020, **22**, 100445, DOI: **10.1016/j.coco.2020.100445**.
14 X. Chen, S. Chen, Z. Xu, J. Zhang, M. Miao and D. Zhang, *Green Chem.*, 2020, **22**, 4187–4198, DOI: **10.1039/D0GC01250E**.
15 N. Eid, B. Ameduri and B. Boutevin, *ACS Sustainable Chem. Eng.*, 2021, **9**, 8018–8031, DOI: **10.1021/acssuschemeng.0c09313**.
16 H. Nakajima, P. Dijkstra and K. Loos, *Polymers*, 2017, **9**, 523, DOI: **10.3390/polym9100523**.
17 Y. Zhang, E. Yukiko and I. Tadahisa, *RSC Sustainable*, 2023, **1**, 543–553, DOI: **10.1039/D2SU00140C**.
18 Y. Jin, Z. Lei, P. Taynton, S. Huang and W. Zhang, *Matter*, 2019, **1**, 1456–1493, DOI: **10.1016/j.matt.2019.09.004**.
19 Y. Liu, Z. Yu, B. Wang, P. Li, J. Zhu and S. Ma, *Green Chem.*, 2022, **24**, 5691–5708, DOI: **10.1039/D2GC00368F**.
20 X. Zhao, Y. Long, S. Xu, X. Liu, L. Chen and Y. Z. Wang, *Mater. Today*, 2023, **64**, 72–97, DOI: **10.1016/j.mattod.2022.12.005**.
21 Q. Li, S. Ma, J. Wei, S. Wang, X. Xu, K. Huang, B. Wang, W. Yuan and J. Zhu, *Macromol. Res.*, 2019, **28**, 480–493, DOI: **10.1007/s13233-020-8064-6**.
22 Y. Zhang, F. Ma, L. Shi, B. Lyu and J. Ma, *Curr. Opin. Green Sustainable Chem.*, 2023, **39**, 100726, DOI: **10.1016/j.cogsc.2022.100726**.

23 J. Palmer, O. R. Ghita, L. Savage and K. E. Evans, *Compos. Part A Appl. Sci. Manuf.*, 2009, **40**, 490–498, DOI: **10.1016/j.compositesa.2009.02.002**.
24 T. Deng, Y. Liu, X. Cui, Y. Yang, S. Jia, Y. Wang, C. Lu, D. Li, R. Cai and X. Hou, *Green Chem.*, 2015, **17**, 2141–2145, DOI: **10.1039/C4GC02512A**.
25 T. Liu, L. Shao, B. Zhao, Y. Chang and J. Zhang, *Macromol. Rapid Commun.*, 2022, **43**, 2200538, DOI: **10.1002/marc.202200538**.
26 Q. Zhao, L. An, C. Li, L. Zhang, J. Jiang and Y. Li, *Compos. Sci. Technol.*, 2022, **224**, 109461, DOI: **10.1016/j.compscitech.2022.109461**.
27 W. Song, A. Magid, D. Li and K.-Y. Lee, *J. Environ. Manage.*, 2020, **269**, 110766, DOI: **10.1016/j.jenvman.2020.110766**.
28 S. Matsuda, M. Miyake and K. Oshima, *Compos. Struct.*, 2022, **292**, 115603, DOI: **10.1016/j.compstruct.2022.115603**.
29 Z. Lei, H. Chen, C. Luo, Y. Rong, Y. Hu, Y. Jin, R. Long, K. Yu and W. Zhang, *Nat. Chem.*, 2022, **14**, 1399–1404, DOI: **10.1038/s41557-022-01046-4**.
30 X. Wu, P. Hartmann, D. Berne, M. De Bruyn, F. Cuminet, Z. Wang, J. M. Zechner, A. D. Boese, V. Placet, S. Caillol and K. Barta, *Science*, 2024, **384**, 177, DOI: **10.1126/science.adj9989**.
31 C. Jehanno, M. M. Pérez-Madrigal, J. Demarteau, H. Sardon and A. P. Dove, *Polym. Chem.*, 2019, **10**, 172–186, DOI: **10.1039/C8PY01284A**.
32 X. Lu, P. Xie, X. Li, T. Li and J. Sun, *Angew. Chem., Int. Ed.*, 2024, **63**, e202316453, DOI: **10.1002/ange.202316453**.
33 E. Sanchez-Rexach, T. G. Johnston, C. Jehanno, H. Sardon and A. Nelson, *Chem. Mater.*, 2020, **32**, 7105–7119, DOI: **10.1021/acs.chemmater.0c02008**.
34 P. R. Christensen, A. M. Scheuermann, K. E. Loeffler and B. A. Helms, *Nature Chem.*, 2019, **11**, 442–448, DOI: **10.1038/s41557-019-0249-2**.
35 M. A. Alraddadi, V. Chiaradia, C. J. Stubbs, J. C. Worch and A. P. Dove, *Polym. Chem.*, 2021, **12**, 5796–5802, DOI: **10.1039/D1PY00754H**.
36 K. Saito, F. Eisenreich, T. Türel and Ž. Tomović, *Angew. Chem., Int. Ed.*, 2022, **61**, e202211806, DOI: **10.1002/ange.202211806**.
37 T. Türel, K. Saito, I. Glišić, T. Middelhoek and Ž. Tomović, *RSC Appl. Polym.*, 2024, **2**, 385, DOI: **10.1039/D3LP00268C**.
38 T. Türel and Ž. Tomović, *ACS Sustainable Chem. Eng.*, 2023, **11**, 8308–8316, DOI: **10.1021/acssuschemeng.3c00761**.
39 K. Saito, T. Türel, F. Eisenreich and Ž. Tomović, *ChemSusChem*, 2023, **16**, e202301017, DOI: **10.1002/cssc.202301017**.
40 P. Schara, A. M. Cristadoro, R. P. Sijbesma and Ž. Tomović, *Macromolecules*, 2023, **56**, 8866–8877, DOI: **10.1021/acs.macromol.3c01645**.
41 A. Hufendiek, S. Lingier and F. E. Du Prez, *Polym. Chem.*, 2019, **10**, 9–33, DOI: **10.1039/C8PY01219A**.
42 R. Mo, L. Song, J. Hu, X. Sheng and X. Zhang, *Polym. Chem.*, 2020, **11**, 974–981, DOI: **10.1039/C9PY01821B**.
43 X. Xu, S. Ma, J. Wu, J. Yang, B. Wang, S. Wang, Q. Li, J. Feng, S. You and J. Zhu, *J. Mater. Chem. A*, 2019, **7**, 15420–15431, DOI: **10.1039/C9TA05293C**.
44 Y. Liu, F. Lu, L. Yang, B. Wang, Y. Huang and Z. Hu, *ACS Sustainable Chem. Eng.*, 2023, **11**, 1527–1539, DOI: **10.1021/acssuschemeng.2c06322**.
45 H. Feng, D. Jin, S. Wang, J. Hu, J. Dai, S. Yan and X. Liu, *Polym. Adv. Technol.*, 2022, **33**, 1665–1676, DOI: **10.1002/pat.5629**.
46 B. Wang, S. Ma, Q. Li, H. Zhang, J. Liu, R. Wang, Z. Chen, X. Xu, S. Wang, N. Lu, Y. Liu, S. Yan and J. Zhu, *Green Chem.*, 2020, **22**, 1275–1290, DOI: **10.1039/C9GC04020J**.
47 S. Ma, J. Wei, Z. Jia, T. Yu, W. Yuan, Q. Li, S. Wang, S. You, R. Liu and J. Zhu, *J. Mater. Chem. A*, 2019, **7**, 1233–1243, DOI: **10.1039/C8TA07140C**.
48 M. Kuroyanagi, A. Yamaguchi, T. Hashimoto, M. Urushisaki, T. Sakaguchi and K. Kawabe, *Polym. J.*, 2021, **54**, 313–322, DOI: **10.1038/s41428-021-00585-w**.
49 P. K. Dubey, S. K. Mahanth, A. Dixit and S. Changmongkol, *IOP Conf. Ser.: Mater. Sci. Eng.*, 2020, **942**, 012014, DOI: **10.1088/1757-899X/942/1/012014**.
50 X. Su, Z. Zhou, J. Liu, J. Luo and R. Liu, *Eur. Polym. J.*, 2020, **140**, 110053, DOI: **10.1016/j.eurpolymj.2020.110053**.
51 A. Roig, P. Hidalgo, X. Ramis, S. De La Flor and À. Serra, *ACS Appl. Polym. Mater.*, 2022, **4**, 9341–9350.
52 Ö. Dağlar, F. Eisenreich and Ž. Tomović, *Adv. Func. Mater.*, 2024, 2408299, DOI: **10.1002/adfm.202408299**.
53 W. Yang, H. Ding, W. Zhou, T. Liu, P. Xu, D. Puglia, J. M. Kenny and P. Ma, *Compos. Sci. Technol.*, 2022, **230**, 109776, DOI: **10.1016/j.compscitech.2022.109776**.
54 Y. Wang, B. Jin, D. Ye and Z. Liu, *Eur. Polym. J.*, 2022, **162**, 110927, DOI: **10.1016/j.eurpolymj.2021.110927**.
55 H. Memon, H. Liu, M. A. Rashid, L. Chen, Q. Jiang, L. Zhang, Y. Wei, W. Liu and Y. Qiu, *Macromolecules*, 2020, **53**, 621–630, DOI: **10.1021/acs.macromol.9b02006**.
56 V. Froidevaux, C. Negrell, S. Caillol, J.-P. Pascault and B. Boutevin, *Chem. Rev.*, 2016, **116**, 14181–14224, DOI: **10.1021/acs.chemrev.6b00486**.
57 M. Fache, B. Boutevin and S. Caillol, *ACS Sustainable Chem. Eng.*, 2015, **4**, 35–46, DOI: **10.1021/acssuschemeng.5b01344**.
58 P. Schara, A. Cristadoro, R. P. Sijbesma and Ž. Tomović, *ChemSusChem*, 2024, e202401595, DOI: **10.1002/cssc.202401595**.
59 T. Türel, B. Eling, A. M. Cristadoro, T. Mathieu, M. Linnenbrink and Ž. Tomović, *ACS Appl. Mater. Interfaces*, 2024, **16**, 6414–6423, DOI: **10.1021/acsami.3c17416**.
60 T. Liu, J. Peng, J. Liu, X. Hao, C. Guo, R. Ou, Z. Liu and Q. Wang, *Composites, Part B*, 2021, **224**, 109188, DOI: **10.1016/j.compositesb.2021.109188**.
61 B. Wang, S. Ma, S. Yan and J. Zhu, *Green Chem.*, 2019, **21**, 5781–5796, DOI: **10.1039/C9GC01760G**.
62 H. Zhang, D. Wang, W. Liu, P. Li, J. Liu, C. Liu, J. Zhang and N. Zhao, *J. Polym. Sci. A*, 2017, **55**, 2011–2018, DOI: **10.1002/pola.28577**.